LAWRENCE
LIVERMORE
NATIONAL
LABORATORY

UCRL-CONF-222467

LOW AMPLITUDE SINGLE AND MULTIPLE SHOCK INITIATION EXPERIMENTS AND MODELING OF LX-04

Kevin S. Vandersall, Craig M. Tarver, Frank Garcia, Steven Chidester, Paul A. Urtiew, Jerry W. Forbes

June 28, 2006

13th International Detonation Sympsosium
Norfolk, VA, United States
July 23, 2006 through July 28, 2006

LOW AMPLITUDE SINGLE AND MULTIPLE SHOCK INITIATION EXPERIMENTS AND MODELING OF LX-04

Kevin S. Vandersall[1], Craig M. Tarver[1], Frank Garcia[1], Steven K. Chidester[1], Paul A. Urtiew[1], and Jerry W. Forbes[2]

[1]Energetic Materials Center, Lawrence Livermore National Laboratory, Livermore, CA 94550
[2]Center for Energetic Concepts Development, University of Maryland, College Park, MD 20742

Abstract. Shock initiation experiments were performed on the plastic bonded explosive (PBX) LX-04 (85% HMX, 15% Viton binder) using single and multiple low amplitude shocks to obtain pressure history data for use in Ignition and Growth reactive flow modeling parameterization. A 100 mm diameter propellant driven gas gun was utilized to initiate the LX-04 explosive charges containing manganin piezoresistive pressure gauge packages placed between explosive discs. In the single shock experiments, the run distances to detonation at three shock pressures showed agreement with previously published data above 3 GPa. Even longer run distances to detonation were measured using 80 mm long by 145 mm diameter LX-04 charges impacted by low velocity projectiles from a 155 mm diameter gun. The minimum shock pressure required to cause low levels of exothermic reaction were determined for these large LX-04 charge dimensions. Multiple shocks were generated as double shocks by using a flyer plate with two materials and as reflected shocks by placing a high impedance material at the rear of the explosive charge. In both cases, the first shock pressure was not high enough to cause detonation of LX-04, and the second shock pressure, which would have been sufficient to cause detonation if generated by a single shock, failed to cause detonation. Thus LX-04 exhibited shock desensitization over a range of 0.6 to 1.4 GPa. The higher shock pressure LX-04 model was extended to accurately simulate these lower pressure and multiple shock gauge records. The shock desensitization effects observed with multiple shock compressions were partially accounted for in the model by using a critical compression corresponding to a shock pressure of 1.2 GPa. This shock desensitization effect occurs at higher pressures than those of other HMX-based PBX's containing higher HMX percentages.

INTRODUCTION

Interest exists in studying safety to shock impact of HMX (octahydro-1,3,5,7-tetranitro-1,3,5,7-tetrazocine) based explosives[1-4]. These prior shock initiation experiments have been performed using wedge tests[1,2], embedded electromagnetic velocity (EMV) particle velocity gauges[3] , and also manganin piezoresistive pressure gauges[4-6]. LX-04 (85% HMX, 15% Viton) has also been studied extensively, including shock initiation behavior at ambient and elevated temperatures. In this paper, the shock sensitivity of LX-04 was measured in single shock, reflected shock, and double shock cases using embedded manganin pressure gauges.

All of these single and multiple shock scenarios can occur during accidents. To give reliable shock sensitivity predictions for other scenarios that cannot be tested directly, the Ignition and Growth reactive flow model parameters must be fitted to all of these types of experimental data. Basically, this combined experimental and reactive

flow modeling effort showed that LX-04 is considerably less sensitive under shock hazard conditions than plastic bonded explosives containing greater than 90% HMX.

EXPERIMENTAL PROCEDURE

Shock initiation experiments were performed on the explosive LX-04 using the 101 mm diameter propellant driven gas gun at the Lawrence Livermore National Laboratory (LLNL) main site or a 155 mm diameter smooth bore Howitzer gun located at LLNL Site 300 (bunker 850). Figure 1 shows a description of a typical experiment. The projectile consisted of a polycarbonate sabot with a 6061-T6 Aluminum flyer plate on the impact surface. Figures 2 and 3 show similar arrangements for measuring reflected as well as double shocks, respectively.

The explosive was in the form of thin disks with gauge packages inserted in between with the total explosive thickness ranging as high as 80 mm for the 155 mm gun cases. For the experiments performed on the 101 mm gun, the explosive discs were 90 mm in diameter and either 5 or 10 mm thick stacked to the final thickness. Likewise, the 155 mm gun experiments used 145 mm diameter discs by 10 mm thickness. The manganin piezoresistive foil pressure gauges placed within the explosive sample were "armored" with sheets of Teflon insulation on each side of the gauge. Manganin is a copper-manganese alloy that changes electrical resistance with pressure (i.e. piezoresistive). Also used were PZT Crystal pins to measure the projectile velocity and tilt (planarity of impact). During the experiment, oscilloscopes measure change of voltage as result of resistance change in the gauges which were then converted to pressure using the hysteresis corrected calibration curve published elsewhere[5,6].

From the data of the shock arrival times of the gauge locations, a plot of distance vs. time ("x-t plot") is constructed with the slope of the plotted lines yielding the shock velocities with two lines apparent, a line for the un-reacted state as it reacts and a line representing the detonation velocity. The intersection of these two lines is taken as the "run-distance-to-detonation," which is then plotted on the "Pop-Plot" showing the run-distance-to-detonation as a function of the input pressure in log-log space.

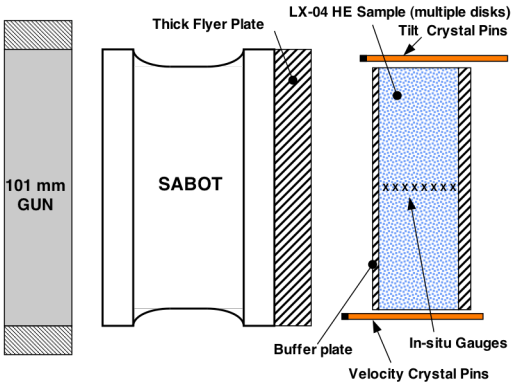

Figure 1. A schematic diagram for the single shock experiment using LX-04 explosive.

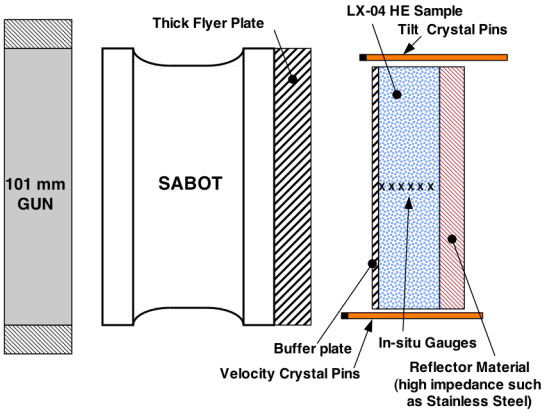

Figure 2. Schematic diagram for the reflected shock experiments with a stainless steel reflector at the back of the target.

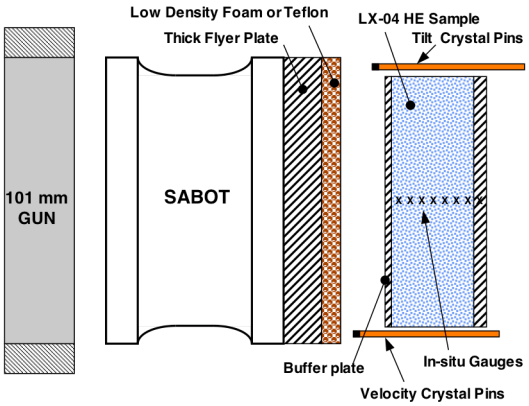

Figure 3. Schematic diagram for the double shock experiments with a flyer composed of two different materials.

Table 1. Listing of Shock Initiation Gun Experiments.

Shot #	Shock	Velocity (km/s)	Pressure (GPa)	Dist. to Det. (mm)
4617	Single	0.793	2.3	28
4618	Single	0.509	2.6	21
4619	Single	0.636	1.8	>55
H06-01	Single	0.389	1.8	65
H06-02	Single	0.368	1.6	>80
4625	Reflected	0.643	1.8 / 3.3	-
4631	Double	0.504	1.4 / 2.8	-
4632	Double	0.511	0.6 / 2.4	-

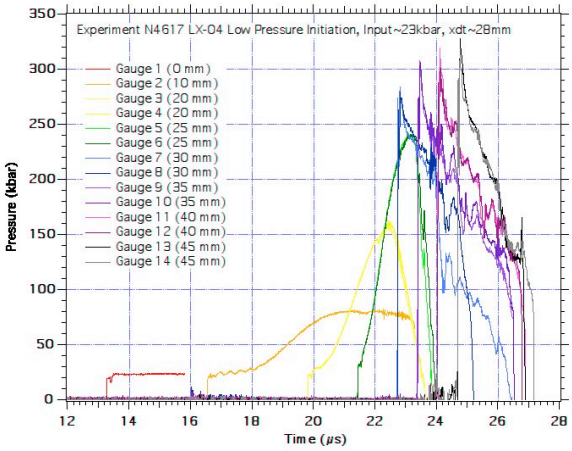

Figure 4. Manganin Gauge records for experiment 4617 showing the initial impact pressure and growth to detonation.

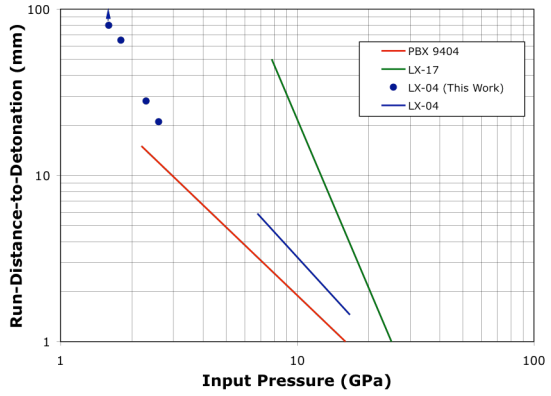

Figure 5. A Pop-plot showing the experimental points for experiments listed in Table 1. Note that PBX9404 and LX-17 lines are also shown for comparison.

EXPERIMENTAL RESULTS

A total of 8 experiments were fired of which 5 had single shocks, 1 involved a reflected shock, and the last two with double shocks. These experimental arrangements were detailed in Figures 1-3. Table 1 displays the impact velocities, pressures generated on impact, and the corresponding run-distance-to-detonation.

A typical gauge record is shown in Figure 4 for experiment 4617 that had a single shock generated by a projectile traveling 793 m/s. This and the other remaining gauge records are displayed in the respective modeling sections where they are compared directly to the modeling results. A "Pop-plot" showing the run-distance-to-detonation points as a function of input pressure is shown in Figure 5. The line for LX-04 from previous experiments as well as PBX9404 and LX-17 for a comparison are shown for comparison to the current data. Note that if the LX-04 line is extrapolated to lower pressure, the two data points with the lower run distance would be included in this trend. However, the two points shown with the longest run distance (one with an arrow showing detonation not observed) seem to indicate that the line curves upward as expected indicating an asymptote reaching a point of no detonation below a threshold velocity.

IGNITION & GROWTH MODELING

The Ignition and Growth reactive flow model for shock initiation and detonation is described in detail in a companion paper.[7] Since the embedded pressure gauges require one-dimensional flow, one-dimensional calculations using a mesh size of 50 zones per mm were used for analysis. Since the current experiments are attempting to measure longer run distances and reaction times, two-dimensional effects did affect some of the gauge records. Thus, converged two-dimensional calculations using 10 zones per mm were used to determine the effects of axial and radial rarefaction waves. Since LX-04 is HMX-based, it exhibits similar hot spot formation and growth rates to other HMX-based explosives, but the greater percentage of binder slows these rates considerably. Ignition and Growth parameters have been previously determined for LX-04 at various initial temperatures and higher shock pressures.[8-11] The

reaction rates for LX-04 under the lower shock pressures used in this study must also correctly calculate the existing high pressure data for ambient temperature LX-04. PBX 9404 (94% HMX with a nitrocellulose based binder) has been shown to undergo shock desensitization at approximately 0.8 GPa,[12] and the gauge records that will be discussed later in the multi-shock section show a similar effect at higher shock pressures for LX-04. Thus a value of 0.0794 for the critical compression parameter was used in the Ignition reaction rate term to prevent ignition below approximately 1.2 GPa. The growth and completion reaction rates are then calibrated to the gauge records. In comparison to previous Ignition and Growth model parameter sets for other HMX-based explosives,[13-15] the LX-04 reaction rates listed in Table 2 create a slower initial growth of the hot spot reactions modeled by the second reaction rate after an ignition of 2% of the LX-04. The third reaction rate models the rapid coalescence of the growing hot spots during the transition to detonation.

SINGLE SHOCK LX-04 MODELING

Figures 6-8 show the calculated and experimental pressure histories in the center zone of each Teflon-coated embedded manganin gauge using the Ignition and Growth parameters for LX-04 listed in Table 2 and the equations of state for the aluminum, Teflon, or steel flyer plates and Teflon gauge packages listed in Table 3 for the three 90 mm diameter targets listed in Table 1 in order of decreasing shock pressure. The measured and calculated reaction growths in Figure 6 agree closely, as the position of the transition to detonation between the 20 and 25 mm deep gauges, for the highest shock pressure experiment number 4618 listed in Table 1. For the intermediate shock pressure experiment 4617, Figure 7 calculated and experimental histories also demonstrate good agreement for the growth of reaction and the transition distance to detonation, which occurs near the 30 mm deep gauge. For the lowest shock experiment number 4619, one-dimensional calculations predict a run distance to detonation of approximately 50mm, whereas the experimental manganin gauge records in Figure 8 show only slow growth of reaction before gauge stretching begins. The two-dimensional calculations shown in Figure 8 confirm that the radial rarefaction limits reaction growth to approximately 4 GPa are in good agreement with the pressure gauges. Therefore the 101 mm gun and corresponding 90 mm diameter charges could only yield one-dimensional run distances up to about 40 mm.

The 155 mm gun was then used with 80 mm long LX-04 charges to obtain the required longer run distances. Figure 9 shows the nine calculated pressures histories for the higher-pressure shot H06-01 in which an aluminum flyer impacted LX-04 at 389 m/s. The calculations show a transition to detonation, which occurs between the 70 mm and 80 mm deep gauges, in good agreement with the experimental transition just before the 70 mm deep gauge. The calculations for the lower shock pressure 155 mm gun shot with an aluminum flyer velocity of 368 m/s resulted in little growth of reaction and no transition to detonation, in good agreement with the experimental result. These LX-04 parameters also predict the previously published pressure histories above 3 GPa and run distances to detonation below 20 mm. For single sustained shock pulses, these parameters accurately reproduce the experimental above 1.4 GPa.

Table 2. Ignition & Growth parameters used for LX-04 modeling.

UNREACTED JWL	PRODUCT JWL
A=9522.0 Mbar	A=15.3516 Mbar
B=-0.05944 Mbar	B=0.6004Mbar
R_1=14.1	R_1=5.1
R_2=1.41	R_2=2.1
ω=0.8867	ω=0.45
C_V=2.7806x10^{-5} Mbar/K	C_V=1.0x10^{-5} Mbar/K
T_o = 298ºK	E_o=0.095 Mbar
Shear Modulus=0.0474 Mbar	-
Yield Strength=0.002 Mbar	-
ρ_0=1.868 g/cm^3	-
REACTION RATES	
a=0.0794	x=4.0
b=0.667	y=2.0
c=0.667	z=3.0
d=0.667	F_{igmax}=0.02
e=0.333	F_{G1max}=0.5
g=1.0	F_{G2min} =0.5
I=2.0 x 10^4 μs^{-1}	G_1=220 Mbar^{-2}μs^{-1}
-	G_2=320 Mbar^{-2}μs^{-1}

Table 3. Gruneisen equation of state parameters for inert materials using the following equation: $P = \rho_0 c^2 \mu[1+(1-\gamma_0/2)\mu - a/2\mu^2]/[1-(S_1-1)\mu - S_2\mu^2/(\mu+1) - S_3\mu^3/(\mu+1)^2]^2 + (\gamma_0 + a\mu)E$, where $\mu = (\rho/\rho_0 - 1)$ and E is thermal energy.

INERT	ρ_0 (g/cm^3)	C (mm/μs)	S_1	S_2	S_3	g_0	a
Al 6061	2.703	5.24	1.4	0.0	0.0	1.97	0.48
Teflon	2.15	1.68	1.123	3.983	-5.797	0.59	0.0
Steel	7.90	4.57	1.49	0.0	0.0	1.93	0.5
Foam	0.80	-1.13	3.77	0.0	0.0	0.20	0.0

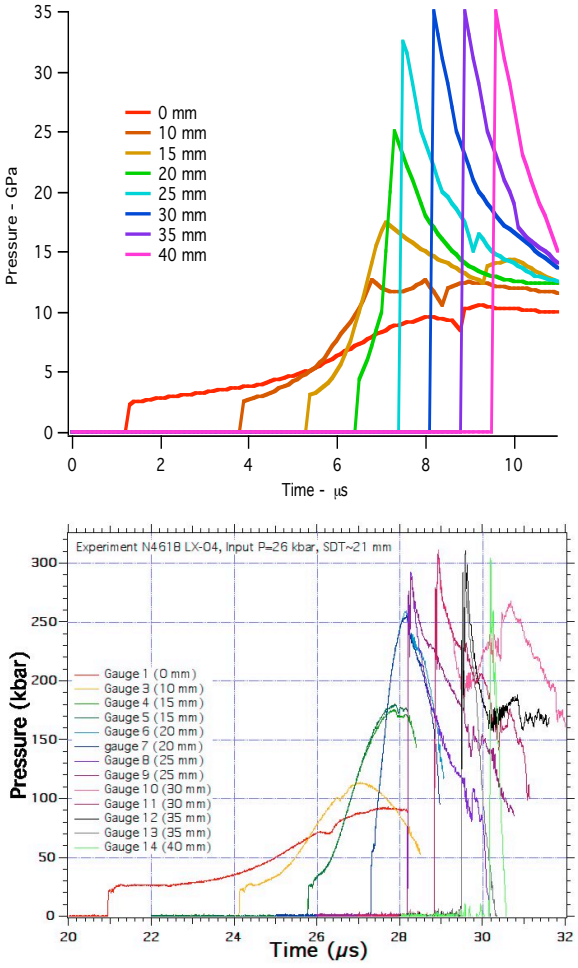

Figure 6. Calculated (top) and experimental (bottom) pressure histories for LX-04 impacted by a steel flyer at 0.509 km/s.

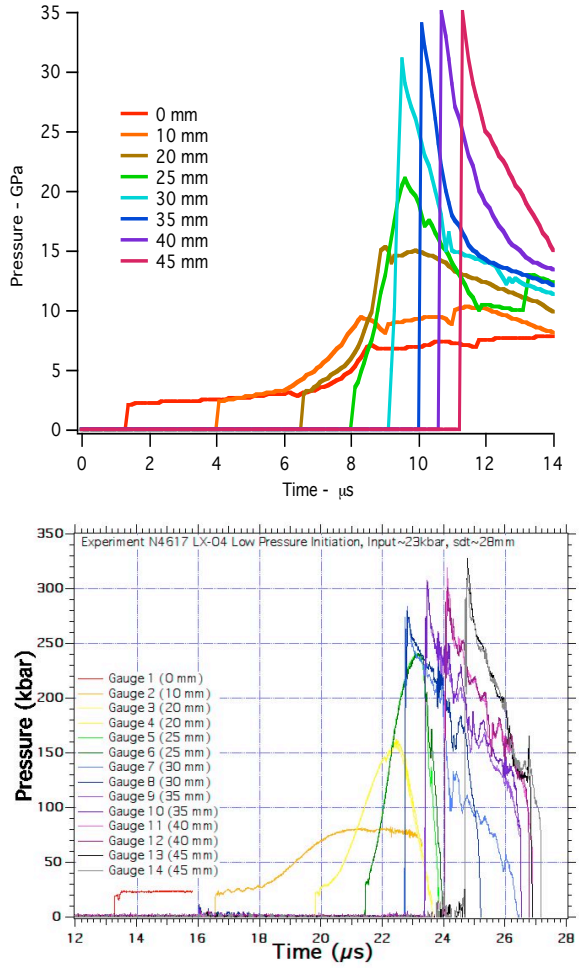

Figure 7. Calculated (top) and experimental (bottom) pressure histories for LX-04 impacted by a Teflon flyer at 0.793 km/s.

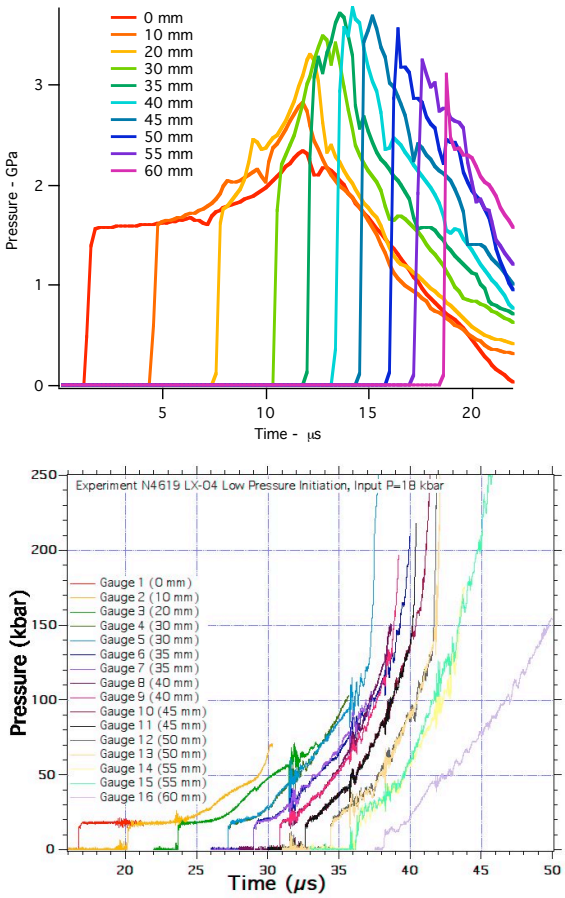

Figure 8. 2D calculated (top) and experimental (bottom) pressure histories for LX-04 impacted by a Teflon flyer at 0.636 km/s.

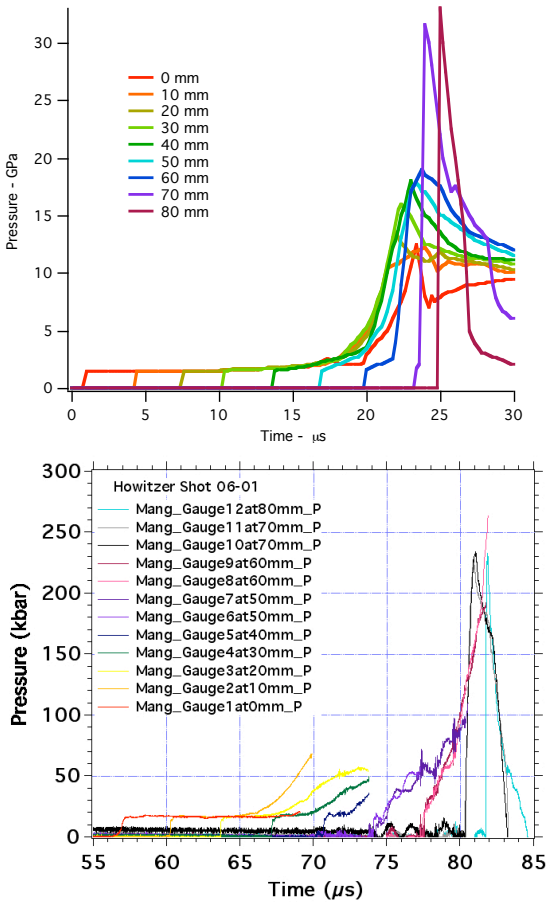

Figure 9. Calculated (top) and experimental (bottom) pressure histories for LX-04 impacted by an Aluminum flyer at 0.389 km/s.

MULTIPLE SHOCK LX-04 MODELING

Figure 10 shows the six calculated pressure histories for LX-04 undergoing reflected shock compression from a steel back plate following an initial shock compression by a Teflon flyer plate at 642.5 m/s. Two-dimensional calculations showed that the rarefaction wave reaches the gauges in the 12 to 14 ms time regime, slowly the rapid growth of reaction in the reflected shock. This agrees well with the experimental records shown below the calculated results. As for other solid explosives,[16] the Ignition and Growth model calculates the reaction rates resulting from strong shock reflections that do not shock desensitize the charge quite well.

In another test of a possible impact scenario, LX-04 was subjected to double shock compressions by composite flyer plates containing two materials of different impedances. The second material was steel and the two experiments were fired at approximately the same velocity, resulting nearly the same final pressures. As shown in Figures 10 and 11, these two double shock resulted in very different reaction rates behind the second shock front. An experiment with a flyer plate of 0.8 g/cm^3 foam and steel exhibited considerable reaction growth behind the second shock. However, another experiment with a Teflon and steel flyer plate showed very little reaction in spite of the fact the Teflon created a higher shock pressure than foam. This is due to shock desensitization of the solid explosive. The Teflon shock pressure was sufficient to compress and react nearly all of the hot spots,

thus leaving mainly closed and/or reacted spots and fully dense explosive for the second shock to compress. This indicates very little reaction growth can occur because the foam does not compress and react all of the hot spot sites. Therefore, there were some hot spots remaining for the second shock to compress and ignite. The growth rate behind the second shock was lower than that of a single shock to the same pressure, because some hot spot sites were removed and the temperature in the doubly shocked solid was lower than that produced by a single shock to the same pressure.

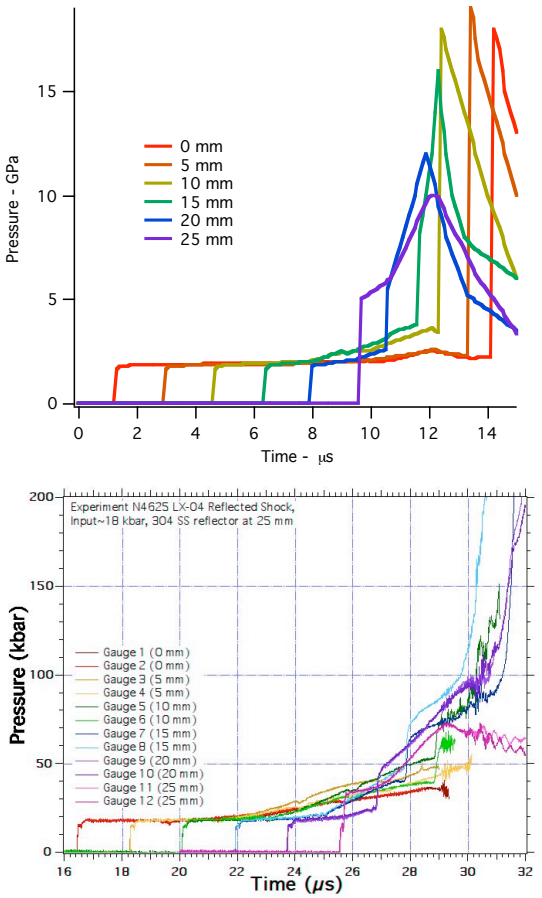

Figure 10. 2D calculated (top) and experimental (bottom) pressure histories for a reflected shock off a stainless steel backing plate behind LX-04 impacted by a Teflon flyer at 0.643 km/s.

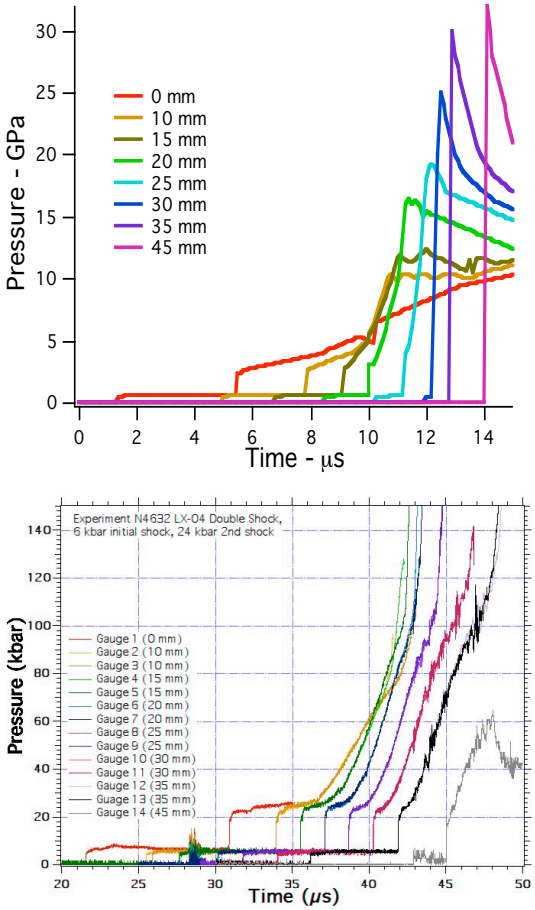

Figure 11. Calculated (top) and experimental (bottom) pressure histories for doubly shocked LX-04 impacted by a foam/steel flyer at 0.511 km/s

Figure 11 shows the calculated pressure histories for the LX-04 double shock experiment with the foam/steel flyer plate. The critical compression parameter prevents reaction in the initial 0.5 GPa pressure shock from foam impact but allows ignition when the second shock arrives. The Ignition and Growth model does eliminate any of the hot spot sites so 2% of the explosive mass reacts when the second shock compression occurs. Thus the Ignition and Growth over-predicts the growth of reaction in Figure 11 and predicts detonation at 45 mm after the second shock overtakes the first. In the experimental data, the gauge records measure considerable reaction following the second shock but no turnover to detonation before the rarefaction wave arrives at the center of the charge. Two-dimensional Ignition and

Growth calculations agree with the one-dimensional curves in Figure 11, and two-dimensional calculations assuming no reaction show that the rarefaction wave arrives at the deeper gauges just after the 14 μs shown in Figure 11.

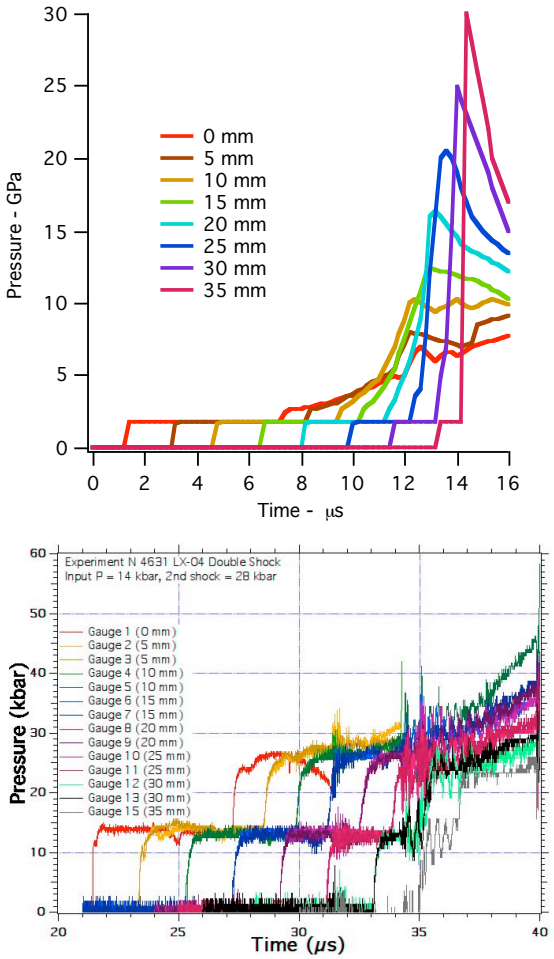

Figure 12. Calculated and experimental pressure histories in doubly shocked LX-04 impacted by a Teflon/steel flyer at 0.504 km/s.

Figure 12 contains the calculated pressure histories for the Teflon/steel double shock experiment that resulted in very little growth of reaction. Again the LX-04 Ignition and Growth parameters prohibit reaction behind the first shock but allow 2% ignition behind the second shock. The subsequent growth of reaction proceeds to high pressures at the deeper gauge positions. The Ignition and Growth again over-predicts reaction rates in this case. This model can be prohibited from further reaction once a specified compression range occurs or have its growth and completion reaction rates frozen at the initial shock values, but theses "fixes" do not account for the physical processes that occur during shock desensitization.

CONCLUSIONS

Embedded manganin pressure gauge records and run distances to detonation were measured for single and multiple shock waves at lower shock pressures for the HMX-based explosive LX-04. These experiments have extended the knowledge of LX-04's reactive flows and runs distance to detonation to pressure regimes that are necessary to understand for many accident scenarios that cannot be tested directly. Additional experiments are planned that simulate other possible scenarios, such as the formation of a Mach stem shock interaction at some depth into the explosive charge. The Ignition and Growth model for LX-04 was extended to these lower pressure results with good agreement under single shock and reflected shock. It over estimated the reaction rates under double shock conditions where complete desensitization occurred. While this is conservative for safety analyses, the more physically based reactive flow Statistical Hot Spot model, which has already successfully calculated shock desensitization in generic HMX- and TATB-based explosives,[17,18] will be applied to this and future LX-04 experimental data. Shock desensitization is a transient phenomena, because it occurs over a relatively small range of shock strengths and durations. When this shock strength and/or duration decreases as a desensitizing shock propagates through an explosive charge, it will no longer have sufficient compression and/or duration to completely destroy the hot spot sites and shock initiation will then become possible again. A great deal of experimental and modeling research is required to understand this complex phenomena.

ACKNOWLEDGEMENTS

The authors would like to thank the 101 mm powder gun crew for all their hard work in obtaining the embedded pressure gauge records. This work was performed under the auspices of the United States Department of Energy by the

University of California, Lawrence Livermore National Laboratory under Contract No. W-7405-ENG-48.

REFERENCES

1. Craig M. Tarver, Paul A. Urtiew, Steven K. Chidester, and LeRoy G. Green, "Shock Compression and Initiation of LX-10," Propellants, Explosives, Pyrotechnics, Vol. 18., pp. 117-127, 1993.

2. A. W. Campbell, W. C. Davis, J. B. Ramsay, and J. R. Travis, "Shock Initiation of Solid Explosives," in the 3rd (International) Symposium on Detonation, September 26-28, Princeton, NJ, 1960, pp. 499-519.

3. LASL Explosive Property Data, Terry R. Gibbs and Alphonse Popolato, Editors, University of California Press, pp. 353-358, 1980.

4. R. L. Gustavsen, S. A. Sheffield, R. R. Alcon, and L. G. Hill, "Shock Initiation of New and Aged PBX 9501," Proceedings of the 12th International Symposium on Detonation, San Diego, CA, August, 2002, p. 530.

5. Vantine, H.C., Erickson, L.M. and Janzen, J., "Hysteresis-Corrected Calibration of Manganin under Shock Loading", J. Appl. Phys., 51 (4), April 1980.

6. Vantine H., Chan J., Erickson L. M., Janzen J., Lee R. and Weingart R. C., "Precision Stress Measurements in Severe Shock-Wave Environments with Low Impedance Manganin Gauges," Rev. Sci. Instr., 51. pp. 116-122 (1980).

7. Tarver, C. M., Lefrancois, A. S., Lee, R. S. and Vandersall, K. S., "Shock initiation of the PETN-based Explosive LX-16," paper presented at this Symposium.

8. Urtiew, P. A., Tarver, C. M., Forbes, J. W., and Garcia, F., "Shock Sensitivity of LX-04 at Elevated Temperatures," Shock Compression of Condensed Matter – 1997, S. C. Schmidt, D. P. Dandekar, and J. W. Forbes, eds., AIP Conference Proceedings 429, AIP Press, New York, 1998, p. 727.

9. Forbes, J. W., Tarver, C. M., Urtiew, P. A., and Garcia, F., "The Effects of Confinement and Temperature on the Shock Sensitivity of Solid Explosives," Eleventh International Detonation Symposium, office of Naval Research ONR 33300-5, Snowmass, CO, 1998, p. 145.

10. Tarver, C. M., Forbes, J. W., Urtiew, P. A., and Garcia, F., "Shock Sensitivity of LX-04 at 150˚C, Shock Compression of Condensed Matter – 1999, M. D. Furnish, L. C. Chhabildas, and R. S. Hixson, eds., AIP Conference Proceedings 505, AIP Press, New York, 2000, p. 891.

11. Urtiew, P. A., Forbew, J. W., Tarver, C. M., Vandersall, K. S., Garcia, F., Greenwood, D. W., Hsu, P. C., and Maienschein, J. L., 'Shock Sensitivity of LX-04 Containing Delta Phase HMX at Elevated Temperatures," Shock Compression of Condensed Matter – 2003, M. D. Furnish, Y. M. Gupta and J. W. Forbes, eds. AIP Conference Proceedings 706, AIP Press, New York, 2004, p. 1053.

12. Campbell, A. W. and Travis, J. R., "The Shock Desensitization of PBX 9404 and Composition B-3," Eighth Symposium (International) on Detonation, Naval Surface Weapons Center NSWC 86-194, Albuquerque, NM, 1985, p. 1057.

13. Tarver, C. M., Hallquist, J. O., and Erickson, L. M., "Modeling Short Pulse Duration Shock Initiation of Solid Explosives," Eighth Symposium (International) on Detonation, Naval Surface Weapons Center NSWC 86-194, Albuquerque, NM, 1985, p. 951.

14. Tarver, C. M., Urtiew, P. A., Chidester, S. K., and Green, L. G., "Shock Compression and Initiation of LX-10," Propellants, Explosives, Pyrotechnics **18**, 117 (1993).

15. Tarver, C. M., Forbes, J. W., Garcia, F., and Urtiew, P. A., "Manganin Guage and Reactive Flow Modeling Study of the Shock Initiation of PBX 9501," Shock Compression of Condensed Matter – 2001, M. D. Furnish, N. N. Thadhani, and Y. Horie, eds., AIP Conference Proceedings 620, AIP Press, New York, 2002, p. 1043.

16. Tarver, C. M., Cook, T. M., Urtiew, P. A., and Tao, W. C., "Multiple Shock Initiation of LX-17," Tenth International Detonation Symposium, Office of the Chief of Naval Research OCNR 33395-12, Boston, MA, 1993, p. 628696.

17. Nichols III, A. L. and Tarver, C. M., "A Statistical Hot Spot Reactive Flow Model for Shock Initiation and Detonation of Solid High Explosives," Twelfth International Detonation Symposium, Office of Naval Research ONR 333-05-2, San Diego, CA, 2002, p. 489.

18. Nichols III, A. L., Tarver, C. M. and McGuire, E. M., "ALE3D Statistical Hot Spot Model Results for LX-17," Shock Compression of Condensed Matter – 2003, M. D. Furnish, Y. M. Gupta and J. W. Forbes, eds. AIP Conference Proceedings 706, AIP Press, New York, 2004, p. 397.